

A hypothetical study on the structural properties of limonene compounds using semi-empirical (PM3) method with arguslab software

Özlem İşcan* 

*Bartın University, Rectorate, Project and Technology Office General Coordination, Bartın, Türkiye

*Corresponding author : oiscan@bartin.edu.tr
Orcid No: <https://orcid.org/0000-0003-3282-1121>

Received : 30/08/2024
Accepted : 12/12/2024

To Cite / Atıf için: İşcan Ö. 2024. A hypothetical study on the structural properties of limonene compounds using semi-empirical (PM3) method with arguslab software. Eurasian J Bio Chem Sci, 7(2):157-164 <https://doi.org/10.46239/ejbc.1558302>

Abstract: Limonene, in its racemic form (+/-), is a naturally occurring cyclic monoterpene and the primary component of citrus peel oil, known for its chemopreventive (cancer-preventive) and antitumor properties. Conformational analysis and geometric optimization of specific limonene derivatives (limonene, carvone, and 4-Methyl-beta-methylenecyclohex-3-en-1-ethyl acetate) were initially performed using ArgusLab 4.0.1 software with PM3 semi-empirical quantum mechanical calculations. Geometries, geometric, and thermodynamic parameters of the compounds were obtained based on their most stable conformations. The geometry energies of the compounds were found to be 62.2637567520 au, -52.6142315455 au, and -84.0390055928 au, respectively. The optimized compounds' HOMO-LUMO frontier orbital energies, molecular electrostatic potential (MEP), solvent surface distribution, UV spectrum values, ZDO and Mulliken charges, as well as dipole moment values, were also calculated using ArgusLab 4.0.1 software.

Keywords: ArgusLab, Limonene, Carvone, PM3, HOMO-LUMO, UV

Arguslab yazılımı ile yarı-empirik (PM3) metodu kullanılarak limonen bileşiklerinin yapısal özellikleri üzerine hipotetik bir çalışma

Özet: Limonen, rasemik formda (+/-), doğal olarak oluşan bir döngüsel monotermen olup, turuncuğil kabuğu yağının birincil bileşenidir ve kemopreventif (kansere önleyici) ve antitümör özellikleriyle bilinir. Belirli limonen bileşiklerinin (limonene, karvon ve 4-Metil-beta-metilen sikloheks-3-en-1-etil asetat) ilk olarak, konformasyon analizi ve geometrik optimizasyonu, ArgusLab 4.0.1 yazılımında PM3 yarı-empirik kuantum mekanik hesaplamaları kullanılarak gerçekleştirilmiştir. Bileşiklerin en kararlı yapıları kullanılarak geometrileri, geometrik ve termodinamik parametreleri elde edilmiştir. Bileşiklerin geometri enerjileri sırasıyla 62.2637567520 au, -52.6142315455 au, ve -84.0390055928 au, bulunmuştur. Optimizasyonu yapılan bileşiklerin HOMO-LUMO sınır orbital enerjileri, moleküler elektrostatik potansiyeli (MEP), çözücü yüzey dağılımı, UV spektrumu değerleri ZDO ve Mulliken yükleri ve dipol moment değeri de ArgusLab 4.0.1 yazılımıyla hesaplanmıştır.

Anahtar Kelimeler: ArgusLab, Limonen, Karvon, PM3, HOMO-LUMO, UV

1. Introduction

ArgusLab is a widely used software in molecular modeling and computational chemistry, supporting various semi-empirical methods to study the electronic properties of molecular structures (Thompson 2004). Through molecular orbital calculations and energy minimization processes, it has the potential to provide insights into the electronic transitions of organic molecules. These electronic transitions, particularly in molecules excited by light absorption in the UV-Vis region, are associated with

transitions from the ground electronic state (S_0) to the excited state (S_1), and are typically dependent on the HOMO-LUMO energy gap (Mortimer 2000). ArgusLab, a computational chemistry software, is commonly used for molecular modelling and drug design, particularly in ligand-receptor interactions. The program provides a graphical user interface (GUI) for building and visualising molecules, running molecular mechanics calculations, and performing semi-empirical quantum chemistry simulations (Laxmi 2014; Ikpeazu and Otuokere 2017; İşcan 2023). PM3 (Parametric Method 3) is a semi-empirical quantum

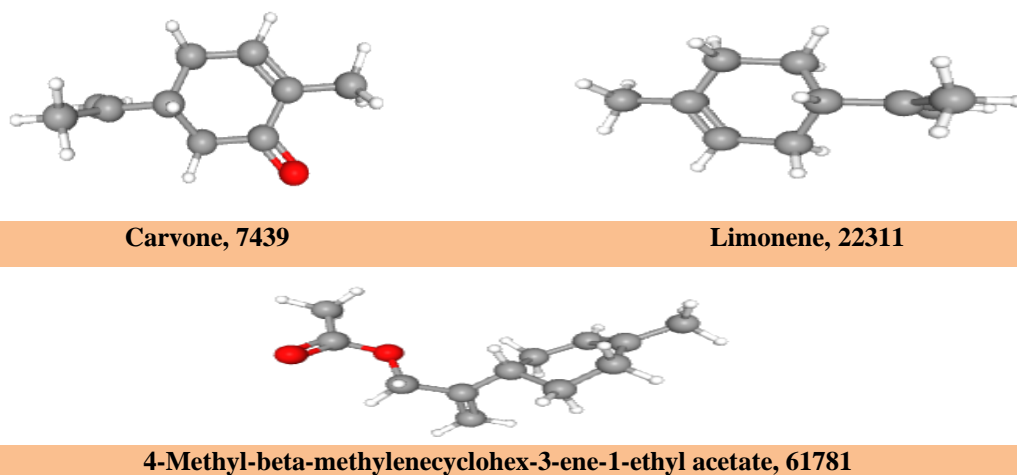


Fig. 1 The names of the compounds and their PubChem ID numbers

chemistry method for studying molecular structures. It was developed to calculate the electronic structure of molecules and is mainly applied to organic molecules for determining energy levels, binding energies, and molecular orbital analyses (Laxmi 2016). DFT calculations for (R)-limonene and (S)-limonene revealed that the HOMO-LUMO energy gaps are 6.679 eV and 6.705 eV, respectively, and that UV absorption is associated with transitions from HOMO to LUMO, indicating that the two enantiomers exhibit comparable reactivity and stability (EL Quafy et al. 2021). The 2D representations of the compounds obtained from PubChem are shown in Fig. 1.

2. Materials and Method

ArgusLab software was employed on a Windows-based computer for all conformational analysis and geometry optimization research. Advances in computing have enabled numerous tools for model building, structure minimization, and molecular representation (Martin 1998; Cruciani et al. 1998; Dunn and Hopfinger 1998). After generating the compound's structure with ArgusLab, the semi-empirical Parametric Method 3 (PM3) parameterization was used to complete the minimization process (Dewar et al. 1985; James and Stewart 1989). The minimum potential energy was calculated using the

geometry convergence function in ArgusLab software. The generated surfaces were designed to illustrate properties of both the ground state and excited states, including orbitals, electron densities, spin densities, and electrostatic potentials (ESP). Grid data were also produced to create molecular orbital surfaces, which depict the molecular orbitals and map the electrostatic potential onto the electron density surface. The geometry convergence map was utilized to determine the minimum potential energy of limonene derivatives (Thomson 1994, 1995, 1996) Finally, the solvent-accessible surface and UV-visible spectra were generated using the ArgusLab software.

3. Results and Discussion

Using the ArgusLab program with the PM3 method, geometry optimization, HOMO-LUMO, MEP (molecular electrostatic potential) energies, UV, and solvent-accessible surface area calculations were performed sequentially on the compounds. Tables 1, 2 and 3 provide the atomic input data for the computation above.

The minimum geometrical energy and SCF energy values calculated using ArgusLab 4.0's RHF/PM3 method are detailed in Tables 4, 5 and 6. Table 7 presents the final minimum geometrical energy and SCF energy values

Table 1 Atomic coordinates of 7439 compound

Atoms No	x	y	z	Atoms No	x	y	z
1O	2.058974	1.907818	-0.208963	14H	-0.499955	2.034432	0.046527
2C	-0.901563	-0.071314	-0.32127	15H	-0.839892	-2.235162	-0.494763
3C	-0.098907	1.046649	0.347208	16H	-0.650306	-1.652885	1.166001
4C	-0.366369	-1.439868	0.11378	17H	1.530653	-2.545856	-0.024922
5C	-2.371389	0.05708	-0.011295	18H	-2.988732	1.157925	-1.73915
6C	1.375139	0.923327	0.001594	19H	-3.168828	-0.600755	-1.884998
7C	1.113644	-1.530508	0.001868	20H	-4.319363	0.330788	-0.908441
8C	1.9255	-0.46404	-0.047952	21H	3.711691	-1.668344	-0.194286
9C	-3.261803	0.24575	-1.190597	22H	3.904055	-0.149202	0.701324
10C	3.401657	-0.615646	-0.156851	23H	3.775796	-0.123568	-1.065066
11C	-2.854127	0.008122	1.230245	24H	-3.91346	0.101883	1.452822
12H	-0.760971	0.020803	-1.427418	25H	-2.22442	-0.12661	2.106436
13H	-0.206026	0.998182	1.450167				

Table 2 Atomic coordinates of 22311 compound

Atoms number	x	y	z	Atoms number	x	y	z
1C	0.719	-0.043	-0.366	14H	0.347	2.043	-0.748
2C	0.042	-1.208	0.353	15H	0.333	1.665	0.967
3C	0.038	1.284	-0.018	16H	-1.936	-1.968	0.697
4C	-1.441	-1.299	-0.017	17H	-1.54	-1.757	-1.009
5C	-2.14	0.038	-0.038	18H	-2.0	2.14	-0.019
6C	-1.46	1.197	-0.022	19H	-3.979	-0.542	-0.97
7C	2.167	0.006	0.013	20H	-4.078	1.001	-0.11
8C	-3.639	-0.002	-0.08	21H	-4.031	-0.511	0.807
9C	3.15	-0.17	-1.107	22H	3.007	-1.142	-1.59
10C	2.563	0.197	1.28	23H	3.016	0.617	-1.857
11H	0.624	-0.208	-1.448	24H	4.187	-0.122	-0.757
12H	0.113	-1.096	1.444	25H	3.617	0.23	1.536
13H	0.532	-2.158	0.105	26H	1.861	0.323	2.097

Table 3 Atomic coordinates of 61781 compound

Atoms number	x	y	z	Atoms number	x	y	z
1O	-2.287	-0.291	0.224	17H	1.245	1.531	-1.819
2O	-4.259	-0.195	-0.976	18H	0.509	-0.872	1.665
3C	0.597	0.416	-0.064	19H	1.368	0.628	1.986
4C	1.675	1.12	-0.896	20H	3.659	0.751	-1.626
5C	1.21	-0.148	1.228	21H	2.491	-0.489	-2.083
6C	2.812	0.16	-1.258	22H	2.89	-1.454	1.827
7C	3.256	-0.713	-0.112	23H	-2.643	1.719	-0.053
8C	-0.542	1.341	0.244	24H	-1.825	0.899	-1.401
9C	2.53	-0.831	1.013	25H	4.802	-2.07	0.564
10C	-1.889	0.965	-0.308	26H	5.372	-0.733	-0.445
11C	4.552	-1.444	-0.299	27H	4.496	-2.095	-1.178
12C	-0.364	2.462	0.959	28H	-1.193	3.13	1.169
13C	-3.502	-0.758	-0.196	29H	0.605	2.751	1.351
14C	-3.788	-2.084	0.442	30H	-3.822	-1.972	1.528
15H	0.225	-0.431	-0.659	31H	-3.021	-2.807	0.153
16H	2.101	1.968	-0.344	32H	-4.76	-2.45	0.098

Table 4 SCF is performed by computing SCF using a single electron matrix. (for 7439).

Cycle	Energy (au)	Difference	Cycle	Energy (au)	Difference	Cycle	Energy (au)	Difference
1	-28.421599		15	-61.618344575	-0.94631	29	-62.26375675	-1.71912e-09
2	-42.042046254	-13.6204	16	-62.184404656	-0.56606	30	-62.263756751	-8.38327e-10
3	-35.39518615	6.64686	17	-62.263291329	-0.0788867	31	-62.263756752	-4.1905e-10
4	-48.633214241	-13.238	18	-62.263682109	-0.00039078	32	-62.263756752	-2.1214e-10
5	-49.287915631	-0.654701	19	-62.263741203	-5.90934e-05	33	-62.263756752	-1.08344e-10
6	-48.939737512	0.348178	20	-62.263751879	-1.06761e-05	34	-62.263756752	-5.28075e-11
7	-50.153658701	-1.21392	21	-62.263755358	-3.47896e-06	35	-62.263756752	-3.10365e-11
8	-51.518937971	-1.36528	22	-62.263756196	-8.3808e-07	36	-62.263756752	-1.54614e-11
9	-52.886295528	-1.36736	23	-62.26375656	-3.64217e-07	37	-62.263756752	-8.35598e-12
10	-53.336277249	-0.449982	24	-62.263756675	-1.14928e-07	38	-62.263756752	-2.67164e-12
11	-54.270082974	-0.933806	25	-62.263756719	-4.39574e-08	39	-62.263756752	-2.38742e-12
12	-55.344065994	-1.07398	26	-62.263756737	-1.80694e-08	40	-62.263756752	-1.98952e-12
13	-57.801898402	-2.45783	27	-62.263756745	-7.88867e-09	41	-62.263756752	-4.54747e-13
14	-60.672034561	-2.87014	28	-62.263756749	-3.61348e-09	42	-62.263756752	-1.13687e-13

Table 5 SCF is performed by computing SCF using a single electron matrix. (for 22311).

Cycle	Energy (au)	Difference	Cycle	Energy (au)	Difference	Cycle	Energy (au)	Difference
1	-21.768358		12	-52.614096137	-0.000848019	23	-52.614231545	-8.82039e-10
2	-33.511036521	-11.7427	13	-52.614182752	-8.66152e-05	24	-52.614231545	-2.72507e-10
3	-33.687344085	-0.176308	14	-52.614219586	-3.68342e-05	25	-52.614231545	-1.21929e-10
4	-40.157009475	-6.46967	15	-52.614227839	-8.25274e-06	26	-52.614231545	-3.7403e-11
5	-42.170399431	-2.01339	16	-52.614230464	-2.62523e-06	27	-52.614231545	-1.37561e-11
6	-43.695639593	-1.52524	17	-52.614231212	-7.47557e-07	28	-52.614231546	-5.11591e-12
7	-46.555932456	-2.86029	18	-52.61423144	-2.28267e-07	29	-52.614231546	-2.27374e-12
8	-51.301611257	-4.74568	19	-52.614231512	-7.13664e-08	30	-52.614231546	-4.54747e-13
9	-52.388557151	-1.08695	20	-52.614231534	-2.2776e-08	31	-52.614231546	-3.97904e-13
10	-52.594216425	-0.205659	21	-52.614231541	-7.01203e-09	32	-52.614231546	5.68434e-14
11	-52.613248118	-0.0190317	22	-52.614231544	-2.75202e-09			

Table 6 SCF is performed by computing SCF using a single electron matrix. (for 61781).

Cycle	Energy (au)	Difference	Cycle	Energy (au)	Difference	Cycle	Energy (au)	Difference
1	-35.146201		16	-83.944417148	-0.576523	30	-84.039005592	-1.39846e-09
2	-56.182071326	-21.0359	17	-84.034575127	-0.090158	31	-84.039005593	-5.06247e-10
3	-50.861912527	5.32016	18	-84.03877621	-0.00420108	32	-84.039005593	-1.74964e-10
4	-60.508370615	-9.64646	19	-84.038930063	-0.000153853	33	-84.039005593	-7.57154e-11
5	-65.780687604	-5.27232	20	-84.038980106	-5.00423e-05	34	-84.039005593	-2.4329e-11
6	-68.604417017	-2.82373	21	-84.038997209	-1.71035e-05	35	-84.039005593	-9.89075e-12
7	-71.524265504	-2.91985	22	-84.039002699	-5.48981e-06	36	-84.039005593	-3.41061e-12
8	-73.109617973	-1.58535	23	-84.039004582	-1.8826e-06	37	-84.039005593	-1.13687e-12
9	-72.822269136	0.287349	24	-84.039005212	-6.30205e-07	38	-84.039005593	-1.59162e-12
10	-71.184165227	1.6381	25	-84.039005462	-2.49744e-07	39	-84.039005593	3.41061e-13
11	-71.084101598	0.100064	26	-84.039005546	-8.44531e-08	40	-84.039005593	9.09495e-13
12	-72.712369973	-1.62827	27	-84.039005576	-3.00626e-08	41	-84.039005593	-3.41061e-13
13	-74.735430973	-2.02306	28	-84.039005587	-1.07466e-08	42	-84.039005593	-9.09495e-13
14	-79.976575556	-5.24114	29	-84.039005591	-3.87865e-09	43	-84.039005593	0.0
15	-83.367893881	-3.39132						

Table 7 compounds' final minimum geometrical energy and SCF energy values.

Compound Number	7439	22311	61781
Final SCF Energy	-62.2637567520 au	-52.6142315455 au	-84.0390055928 au
Final SCF Energy	-39071.1325 kcal/mol	-33015.9585 kcal/mol	-52735.3198 kcal/mol

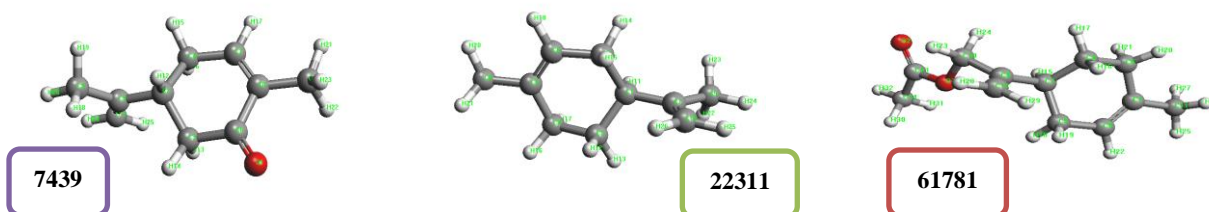
**Fig. 2** Optimized structures of the compound

Table 8. Ground State Dipole (debye)

Comp. Number	X	Y	Z	length
7439	-1.74523919	-2.42399485	0.30117895	3.00205257
22311	-0.06869694	-0.19994140	-0.22845694	0.31126902
61781	1.12243970	-0.65112639	1.28898502	1.82902128

The geometry of the compounds was optimized using the PM3 method in the ArgusLab program. The optimized structures of the compounds are presented in Fig. 2. These structures represent the lowest energy configurations, providing insight into the molecular geometry and interactions within the compounds.

Mulliken and ZDO (Zero Differential Overlap) atomic charges are two essential approaches used to calculate the distribution of charges on atoms in molecular systems. Mulliken charges are based on the distribution of molecular orbitals across atoms to calculate charges. While the Mulliken method offers a simple and understandable approach to calculating atomic charges, it can sometimes lead to non-physical results, such as negative charges (Mulliken 1955). On the other hand, ZDO atomic charges stand out as a more suitable method, particularly for larger and more complex systems. ZDO simplifies the calculation process by neglecting differences in integrals, thus yielding more balanced results (Foster 1980). These methods are frequently used tools for researchers looking to analyse molecular charge distribution in quantum chemistry.

Table 9 List of Mulliken and ZDO Atomic Charges of 7439 by using ArgusLab software

Atoms No	ZDO Atomic Charges	Mulliken Atomic Charges	Atoms No	ZDO Atomic Charges	Mulliken Atomic Charges
1O	-0.3143	-0.3251	14H	0.0824	0.1607
2C	-0.029	-0.1011	15H	0.0642	0.1378
3C	-0.1528	-0.3097	16H	0.0701	0.1412
4C	-0.0747	-0.2150	17H	0.1026	0.1894
5C	-0.1157	-0.1278	18H	0.0489	0.1166
6C	0.3220	0.3506	19H	0.0465	0.1136
7C	-0.0843	-0.1721	20H	0.0452	0.1128
8C	-0.1903	-0.2154	21H	0.0391	0.1051
9C	-0.0706	-0.2670	22H	0.0524	0.1225
10C	-0.0571	-0.2534	23H	0.0573	0.1286
11C	-0.1654	-0.3290	24H	0.0876	0.1729
12H	0.0734	0.1476	25H	0.0850	0.1664
13H	0.0776	0.1499			

Table 10 List of Mulliken and ZDO Atomic Charges of 22311 by using ArgusLab software

Atoms No	ZDO Atomic Charges	Mulliken Atomic Charges	Atoms No	ZDO Atomic Charges	Mulliken Atomic Charges
1C	-0.0389	-0.1099	14H	0.0550	0.1266
2C	-0.0952	-0.2344	15H	0.0618	0.1319
3C	-0.0553	-0.1917	16H	0.0544	0.1250
4C	-0.0499	-0.1862	17H	0.0549	0.1239
5C	-0.1294	-0.1408	18H	0.0999	0.1866
6C	-0.1497	-0.2380	19H	0.0427	0.1097
7C	-0.1124	-0.1237	20H	0.0412	0.1076
8C	-0.0643	-0.2586	21H	0.0438	0.1103
9C	-0.0692	-0.2657	22H	0.0456	0.1125
10C	-0.1718	-0.3361	23H	0.0457	0.1128
11H	0.0690	0.1414	24H	0.0423	0.1093
12H	0.0571	0.1269	25H	0.0841	0.1686
13H	0.0524	0.1243	26H	0.0861	0.1678

Table 11 List of Mulliken and ZDO Atomic Charges of 61781 by using ArgusLab software

Atoms No	ZDO Atomic Charges	Mulliken Atomic Charges	Atoms No	ZDO Atomic Charges	Mulliken Atomic Charges
1O	-0.2671	-0.2773	17H	0.0520	0.1237
2O	-0.3811	-0.3956	18H	0.0598	0.1330
3C	-0.0332	-0.1048	19H	0.0599	0.1289
4C	-0.0959	-0.2351	20H	0.0551	0.1258
5C	-0.0554	-0.1918	21H	0.0556	0.1246
6C	-0.0494	-0.1858	22H	0.1003	0.1871
7C	-0.1296	-0.1410	23H	0.0499	0.1204
8C	-0.1341	-0.1498	24H	0.0534	0.1236
9C	-0.1498	-0.2382	25H	0.0414	0.1078
10C	0.1186	-0.0144	26H	0.0440	0.1107
11C	-0.0646	-0.2590	27H	0.0430	0.1100
12C	-0.1349	-0.2986	28H	0.0848	0.1696
13C	0.3694	0.3976	29H	0.0867	0.1685
14C	-0.1143	-0.339	30H	0.0684	0.1412
15H	0.0736	0.1481	31H	0.0684	0.1407
16H	0.0557	0.1255	32H	0.0692	0.1442

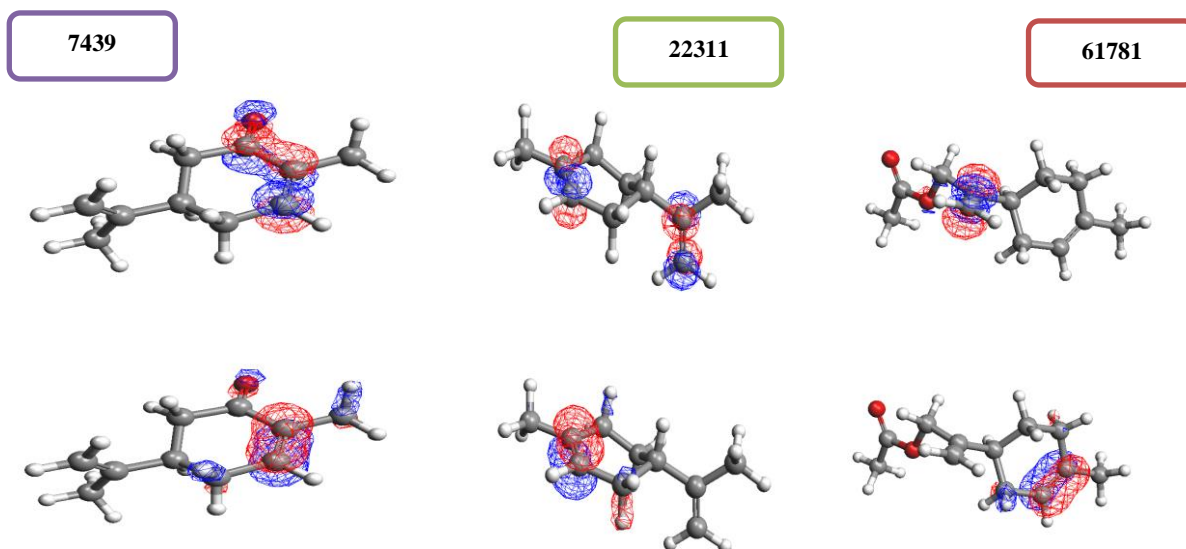


Fig. 3 Visualise the HOMO (a) and LUMO(b) of Compounds; blue shows positive and red shows negative.

ELECTRON DENSITY

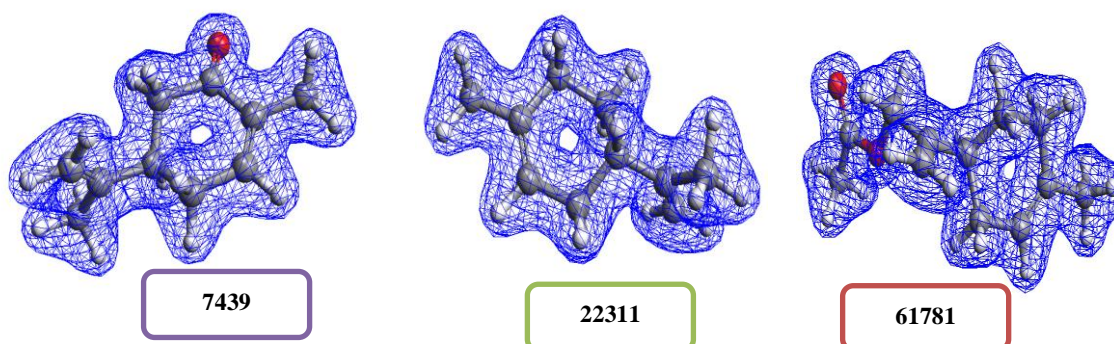


Fig. 4 Electron density representation of compounds

The HOMO-LUMO representations of limonene compound derivatives are shown in Fig. 3. The electron density of limonene compound derivatives is shown in Fig. 4.

An ESP-mapped density surface can illustrate areas within a molecule more susceptible to nucleophilic or electrophilic attack. These surfaces are valuable for qualitative interpretations, highlighting regions where chemical reactivity is likely, as seen in Fig. 5. A colour spectrum ranging between -0.0200 and +0.17 has been used.

Solvent accesibe surface

Solvent Accessible Surface" (SAS) refers to the external surface of a molecule that can interact with solvent molecules. This concept is typically used to study biomolecules' structural and functional properties, such as proteins, and plays a critical role in determining a molecule's interactions with solvents (Richard 1977). SAS calculates how much of a large molecule, like a protein, is accessible to solvent molecules (e.g., water), making it an essential parameter in biological processes. The solvent

accessible surface of the compounds, calculated using ArgusLab, is shown in Fig. 6.

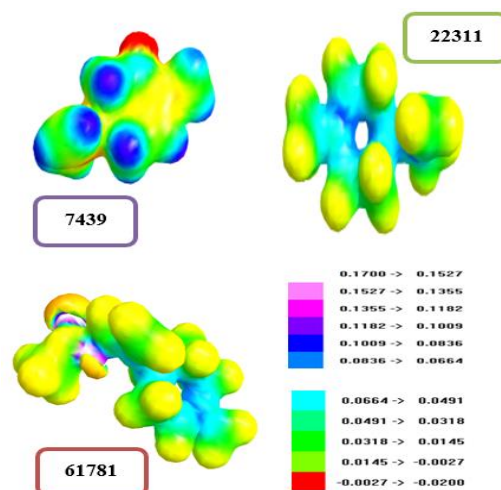


Fig. 5 shows a potential electrostatic map of the terminal molecule produced by applying the Mulliken charges with the scale of compounds

Compounds like limonene derivatives, which are aliphatic hydrocarbons, typically exhibit low UV absorption in UV-visible spectroscopy because they do not contain strong chromophore groups, such as conjugated double bonds. Limonene's UV absorption has been reported to occur mainly between 190–220 nm. This range is typical for simple aliphatic hydrocarbons and is generally attributed to $\pi \rightarrow \pi^*$ transitions (Śmiałek et al. 2012).

Fig. 7 presents limonene derivative compounds' UV/visible electronic absorption spectrum. In the spectrum, intense peaks are observed at 174.1, 183.5, and 171.3 nm, while relatively low-intensity peaks appear at 228.5, 173.7, and 178.3 nm, representing the strength of the transitions of the compound. These values differ from experimental results by approximately 20–30 nm for all peaks, reflecting the challenges in accurately predicting the absorption spectra of these compounds with the currently available computational methods. Since the compounds do not possess UV-active

aromatic rings or large conjugation systems, the absorption peak observed in UV spectra is typically weak.

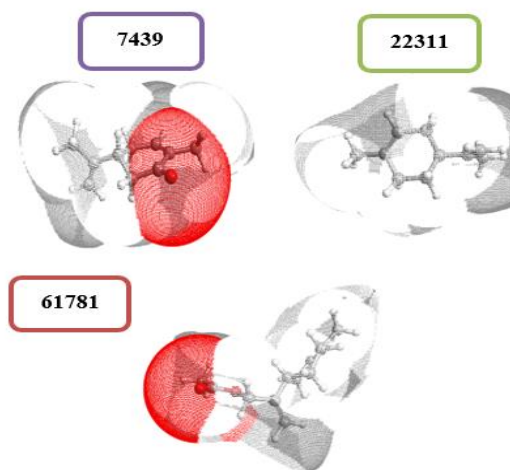


Fig. 6 Solvent-accessible surface of compounds

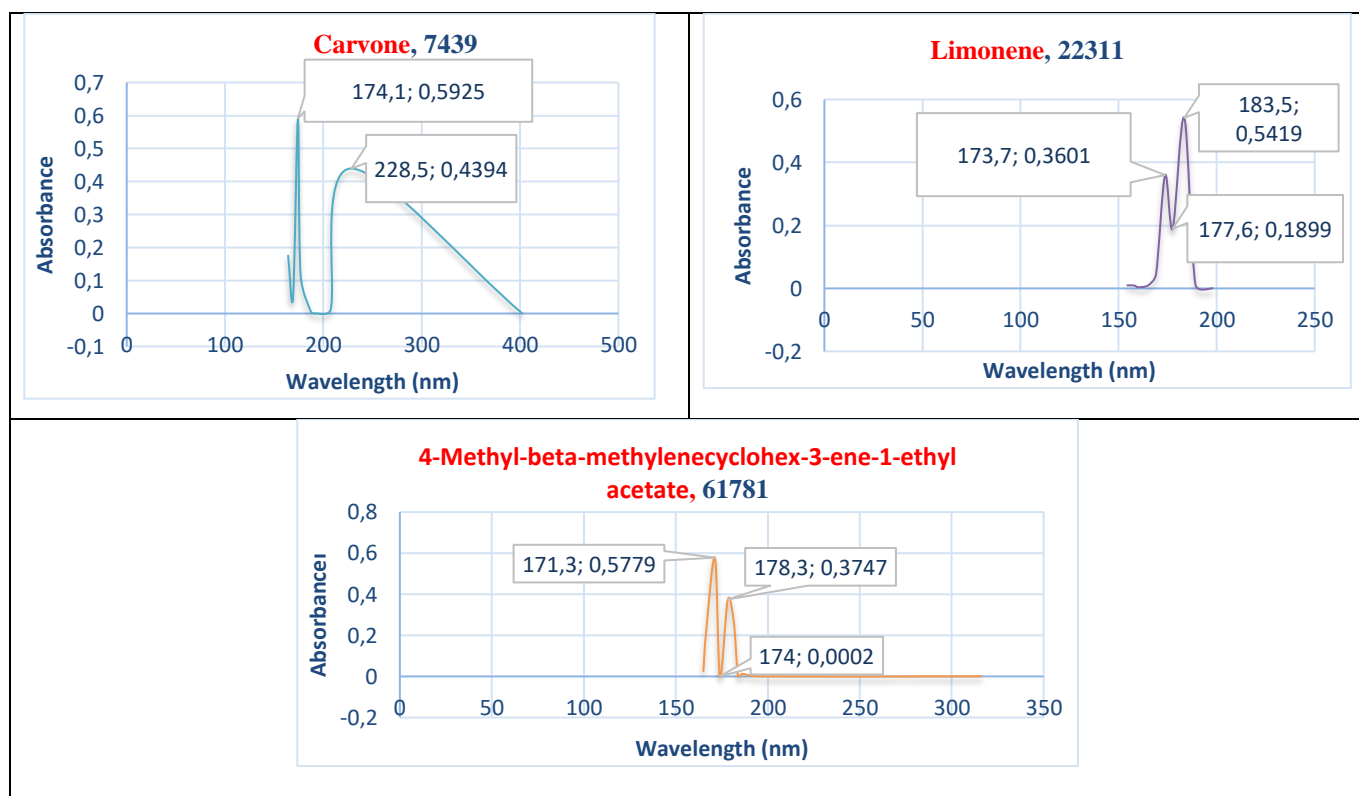


Fig. 7 Electronic absorption spectrum of the compounds

4. Conclusion

It has been observed that the ArgusLab program has a very user-friendly interface and completes calculations in a very short time. In this research study, we included some calculation tasks that can be performed using ArgusLab and observed that the results are stable. Using the ArgusLab software, the lowest energy favorable conformations of limonene compound derivatives were found to be -62.2637567520 au, -52.6142315455 au, and -

84.0390055928 au, respectively. The lowest energy conformations were employed in molecular modeling calculations after the geometric variables related to compounds were finally fully optimized for the compound. The calculated thermodynamic parameter, dipole moment, Mulliken and ZDO Atomic Charge, and optimized geometry were all well within the computational results' accuracy range. The ΔE values for the compounds numbered 7439, 22311, and 61781 are calculated as -

0.005155, -0.382305, and -0.038150, respectively, based on their eigenvalues. Compound 22311, with the largest $\Delta E_{\Delta E}$, exhibits the highest reactivity, while compound 7439, with the smallest $\Delta E_{\Delta E}$, indicates greater stability and lower reactivity, positioning 61781 as intermediate between the two. Azure A and Hyamine, with their narrow HOMO-LUMO energy gaps and active sites revealed through Mulliken charges, demonstrate the importance of computational models in understanding electronic structures for various applications (Özkır et al. 2012, 2013). The compound numbered 7439 appears to have a smaller solvent-accessible surface, indicating a more compact structure or fewer hydrophilic regions exposed to the solvent. In contrast, the compounds numbered 22311 and 61781 possess larger solvent-accessible surfaces, suggesting that their surface characteristics include a higher number of polar or nonpolar regions. This distinction may influence the hydrophilic and hydrophobic properties of the

compounds, as well as their interaction potential with solvents and solubility profiles.

In conclusion, the UV/visible electronic absorption spectrum of limonene derivative compounds, as presented in this study, demonstrates low-intensity peaks, consistent with the characteristics of aliphatic hydrocarbons that lack strong chromophores or large conjugation systems. The observed peaks at 174.1, 183.5, and 171.3 nm, along with weaker peaks at 228.5, 173.7, and 178.3 nm, correspond to $\pi \rightarrow \pi^*$ transitions typical for such compounds. The discrepancies of approximately 20–30 nm between the computational and experimental results highlight the limitations of current computational methods in accurately predicting UV absorption spectra for limonene derivatives. These findings underline the need for further refinement of computational models to enhance the accuracy of spectral predictions for non-aromatic, non-conjugated systems.

References

- Cruciani G, Clementi S, Pastor M. 1998. Golpe guided region selection. *Perspectives in Drug Discovery and Design*. 12-14(16): 71-86.
- Dewar MJS, Zoobisch EG, Healy EF, Stewart JJP. 1985. AM1: A new general purpose quantum mechanical molecular model. *J Am Chem Soc*. 107: 3902-3910.
- Dunn III, Hopfinger AJ. 1998. *Drug Discovery*, Kluwer Academic Publishers. Chapter 12, pp.167-182.
- EL Ouafy, H., EL Ouafy, T., Oubenali, M., EL Haimouti, A., Gamouh, A., & Mbarki, M. (2021). Analysis of the Chemical Reactivity of Limonene by the Functional Density Theory Method Using Global Descriptors. *Journal of Chemical Health Risks*, 11(2), 213-221.
- Foster, JP, Weinhold F. 1980. Natural hybrid orbitals. *J Am Chem Soc*. 102(24), 7211-7218. doi: 10.1021/ja00544a007.
- Ikpeazu OV, Otuokere IE, Igwe KK. 2017. Molecular geometry optimization and frontier molecular orbitals of luminal Na-K-Cl cotransporter (NKCC2) Inhibitor, 5-(aminosulfonyl)-4-chloro-2-[(2-furylmethyl) amino] benzoic acid, furosemide. *J. Environ Life Sci* 2(1), 29-33.
- İşcan Ö. 2023. A Insilico Study on Structural aspects of Caffeine by ArgusLab 4 software. *Journal of Physical Chemistry and Functional Materials*. 6(2):138-144. doi.org/10.54565/jphcfum.1402117.
- Laxmi K. 2014. *Scientia Research Library*. *J Appl Chem*. 2(1): 92-101.
- Laxmi K. 2016. A Hypothetical Study on Structural aspects of Indole-3-carbinol (I3C) by Hyperchem and Arguslab 4 software. *Int Journal of Engineering Research and Applications*. 6(1): 17-24.
- Martin YC. 1998. *Perspective in drug discovery and design*. Springer Publisher, 12th Volume, pp.3- 23.
- Mortimer RG. 2000. *Physical chemistry*. Academic Press.
- Mulliken RS. 1955. Electronic Population Analysis on LCAO–MO Molecular Wave Functions. I. *J Chem Phys* 23(10): 1833-1840. doi: 10.1063/1.1740588.
- Özkır, D., Kayakırılmaz, K., Bayol, E., Gürten, A. A., & Kandemirli, F. (2012). The inhibition effect of Azure A on mild steel in 1 M HCl. A complete study: Adsorption, temperature, duration and quantum chemical aspects. *Corrosion Science*, 56, 143-152.
- Özkır, D., Bayol, E., Gürten, A., Sürme, Y., & Kandemirli, F. (2013). Effect of hyamine on electrochemical behaviour of brass alloy in HNO₃ solution. *Chemical Papers*, 67(2), 202-212.
- Richards FM. 1977. Areas, volumes, packing, and protein structure. *Annu Rev Biophys*, 6(1): 151-176.
- Smialek MA, Hubin-Franskin MJ, Delwiche J, Duflo D, Mason NJ, Vronning-Hoffmann, SALV P, Limao-Vieira P. (2012). Limonene: electronic state spectroscopy by high-resolution vacuum ultraviolet photoabsorption, electron scattering, He (I) photoelectron spectroscopy and ab initio calculations. *Phys Chem Chem Phys*. 14(6), 2056-2064.
- Stewart JJP. 1989. *Comp. Chem.*, 10, 209-220 and 221-264, 1989.
- Thompson MA, Glendening ED, Feller D. 1994. The nature of K⁺/crown ether interactions: A hybrid quantum mechanical-molecular mechanical study. *J Phys Chem*. 98(41):10465-10476.
- Thompson MA, Gregory K, Schenter J. 1995. *Phys Chem*, 99:6374-6386.
- Thompson MA. 1996. QM/MMpol: A consistent model for solute/solvent polarization. Application to the aqueous solvation and spectroscopy of formaldehyde, acetaldehyde, and acetone. *J Phys Chem*. 100(34): 14492-14507.
- Thompson MA. 2004. Molecular docking using ArgusLab, an efficient shape-based search algorithm and the AScoring function. ACS meeting Philadelphia 172:CINF 42, PA.